Enhancing Face Detection Performance in Low-Light Conditions Using NIR Thermal Imaging and Image Morphology

1st Maulisa Oktiana*
Electrical and Computer Eng Dept
Universitas Syiah Kuala
Banda Aceh, Indonesia
maulisaoktiana@usk.ac.id

2nd Cut Salsabilla Azra
Electrical and Computer Eng. Dept
Universitas Syiah Kuala
Banda Aceh, Indonesia
cutsalsabilaazra@gmail.com

3rd Rusdha Muharar
Electrical and Computer Eng. Dept
Universitas Syiah Kuala
Banda Aceh, Indonesia
rusdhamuharrar@usk.ac.id

4th Fajrul Islamy
Electrical and Computer Eng. Dept
Universitas Syiah Kuala
Banda Aceh, Indonesia
fajrulislamy@usk.ac.id

5th Rizka Ramadhana
Electrical and Computer Eng. Dept
Universitas Syiah Kuala
Banda Aceh, Indonesia
rizkaramadhana@usk.ac.id

6th Melinda Melinda
Electrical and Computer Eng. Dept
Universitas Syiah Kuala
Banda Aceh, Indonesia
melinda@usk.ac.id

7th Niza Aulia
Electrical and Computer Eng. Dept
Universitas Syiah Kuala
Banda Aceh, Indonesia
niza@usk.ac.id

8th Muharratul Mina Rizky
Electrical and Computer Eng. Dept
Universitas Syiah Kuala
Banda Aceh, Indonesia
kiky@usk.ac.id

9th Maya Fitria
Electrical and Computer Eng. Dept
Universitas Syiah Kuala
Banda Aceh, Indonesia
mayafitria@usk.ac.id

Abstract—**Face detection plays a vital role in biometric, security, and surveillance systems. Conventional approaches based on the visible light (VIS) spectrum often suffer performance degradation under poor lighting conditions, limiting their reliability. To address this issue, this study employs thermal imagery in the Near-Infrared (NIR) spectrum, which is less affected by ambient light, combined with image morphology operations to enhance segmentation accuracy. Experiments were conducted using the LDHF-DB dataset (300 images at distances of 1 m, 60 m, and 100 m) and a subset of the Tuft dataset (60 images). Face detection was performed using the HOG + SVM method, followed by Otsu thresholding and morphological operations. Performance was evaluated using Peak Signal-to-Noise Ratio (PSNR). Results show that applying morphological operations significantly improves PSNR values, with an average increase of more than 35%. The best performance was achieved on the 1 m subset, while longer distances presented greater challenges. These findings highlight the potential of integrating NIR thermal imagery and morphological processing to improve the robustness and reliability of face detection systems in low-light environments.**

Keywords—**Face detection, Thermal image, NIR spectrum, Image morphology.**

I. INTRODUCTION

In recent years, face recognition has received increasing attention due to its wide applications in biometrics, security, access control, and surveillance systems [1][2]. As a fundamental stage, face detection plays a decisive role since its accuracy directly affects subsequent recognition processes [3]. However, reliable face detection remains challenging in outdoor or semi-outdoor environments where illumination conditions vary significantly. This limitation has restricted most recognition systems to indoor scenarios with controlled lighting [4].

Conventional approaches typically rely on images in the visible light (VIS) spectrum. While VIS-based methods can achieve high accuracy under good illumination, their performance deteriorates in low-light or nighttime conditions [5]. To overcome this limitation, thermal imaging in the Near-Infrared (NIR) spectrum has been explored as an alternative. Unlike VIS images, NIR thermal images are relatively insensitive to lighting variations, enabling consistent detection both in daylight and complete darkness [6][7]. Moreover, the NIR spectrum provides clearer details, penetrates atmospheric disturbances such as fog or haze, and enhances robustness in challenging environments [8].

Several studies have investigated thermal-based face detection. Previous works applied thresholding, skin-color segmentation, or facial geometry analysis to improve detection accuracy [9] [10]. While these methods showed promising results, segmentation errors often persist, leaving non-facial regions unremoved. To address this issue, morphological image processing has been proposed, as it effectively refines segmentation, removes noise, and preserves essential facial structures [11].

Previous research [12] used thermal images to detect frontal faces in various standing body poses. The methods used included thresholding for thermal image segmentation, morphological filters to refine the segmented images, and facial geometry as a discriminative feature based on the size, ratio, and shape of the face. Another study employed morphological methods to detect facial areas in VIS images using the YCbCr color model for skin color segmentation [13]. Research [14] compared thermal face recognition

methods, highlighting their advantages and disadvantages. The advantages of thermal images include their insensitivity to lighting variations, the ability to work in dark conditions, and reduced visibility requirements. However, a notable disadvantage of thermal images is their sensitivity to glass.

Motivated by these findings, this study proposes a face detection approach that integrates NIR thermal imaging with morphological operations to improve segmentation accuracy. The method is evaluated using the LDHF-DB and Tuft datasets at multiple distances, with performance assessed based on the Peak Signal-to-Noise Ratio (PSNR). The main contributions of this study can be summarized as follows:

1. Employing NIR thermal imagery to mitigate illumination-related limitations of VIS-based detection.
2. Applying morphological operations to enhance segmentation results and reduce non-facial artifacts.
3. Providing a quantitative performance analysis using PSNR across different datasets and capture distances.

This work demonstrates the potential of combining NIR spectrum imaging and morphological processing as a robust solution for face detection in low-light and unconstrained environments. The rest of this paper is organized as follows. Section II describes the materials and methods, including the datasets, face detection process, thresholding, morphological operations, and performance evaluation metrics. Section III presents the experimental results and analysis, highlighting the effectiveness of the proposed approach across different datasets and image distances. Section V concludes the paper with key findings and recommendations for future research.

II. METHODS AND MATERIALS

Figure 1 illustrates the overall methodology applied in this study. The process begins with input NIR images, which are then processed by a face detector to identify and localize facial regions. After detection, the images undergo thresholding using Otsu's method to separate the face from the background by converting the grayscale image into a binary format. However, the initial segmentation often still contains non-facial areas or noise. To address this, morphological operations (dilation and closing) are applied to refine the segmentation, remove small holes, and improve the continuity of the facial region. The resulting binary mask is then combined with the original ground-truth facial region through a masking process, ensuring that only the desired face area is retained. Finally, the results are assessed in the evaluation stage using Peak Signal-to-Noise Ratio (PSNR) as the primary metric to measure image quality and detection accuracy. Each stage will be described as follows.
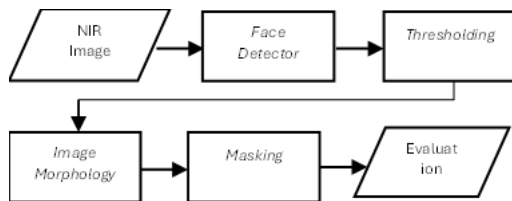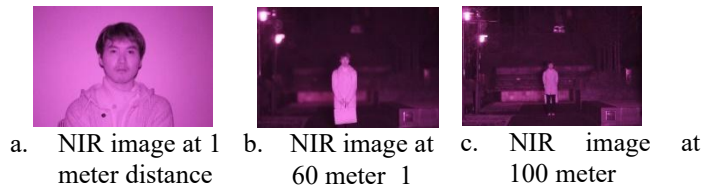

Fig. 1. Research Flow

a. NIR image at 1 meter distance   b. NIR image at 60 meter 1   c. NIR image at 100 meter

Fig. 2. LDHF-DB dataset image

Fig. 3. Tuft dataset image

A. NIR Images Dataset

This study employs two publicly available datasets: the Long-Distance Heterogeneous Face Database (LDHF-DB) [15] and the Tuft dataset [16]. LDHF-DB contains 300 NIR facial images from 100 subjects (70 males and 30 females), captured at distances of 1 m, 60 m, and 100 m. Each image has a resolution of 5184 × 3456 pixels and is available in JPG and RAW formats, with a total dataset size of 1.83 GB. The Tuft dataset consists of 1098 facial images from 40 subjects (32 males and 8 females), with a resolution of 3280 × 2464 pixels and a total size of 14.4 GB. The sample of the LDHF-DB image and the Tuft dataset image are illustrated in Figures 2 and 3, respectively.

In this work, only a subset of 60 images from 6 subjects (4 males and 2 females) was used. The NIR images from both datasets were used as input at different capture distances (1 m, 60 m, and 100 m). Preprocessing included resizing and converting to grayscale before the segmentation and detection steps.

B. Face Detection

Face detection was performed using the Histogram of Oriented Gradients (HOG) combined with a linear Support Vector Machine (SVM) classifier from the *dlib* library [17][18]. The method extracts gradient features, constructs histogram cells, and groups them into blocks for training and classification. The model used, *shape_predictor_68_face_landmarks.dat*, predicts 68 landmark points on the human face. A bounding box was then generated using OpenCV functions (cv2.boundingRect and cv2.rectangle) to localize the detected face region.

C. Thresholding

After detection, images were converted to grayscale and processed using Otsu's thresholding. This method automatically determines the optimal threshold value to segment the image into foreground (face region) and background, producing a binary image for further processing [19]. At this stage, the RGB image is read in grayscale mode. The grayscale image is converted into a binary image, where

the gray level of each pixel is expressed as 0 or 1, depending on its value.

D. Morphological Operations

After going through the thresholding stage, the image then enters the segmentation process using the image morphology method. This stage aims to improve the results of the image segmentation process, as the face detector process still fails to accurately localize parts of the image other than the face. The morphological operations used in this study are:

1. Dilation

The dilation operation aims to expand the foreground (white region), connect disjointed areas, and fill small gaps. In the dilation operation, the foreground (white area) of the image widens, resulting in an output image that is thicker than the original (with a wider white area) [20].

2. Closing

The closing operation aims to fill in small holes in the object segment, smooth the contours, refine the object boundaries, and eliminate smaller holes in the face image object [21].

Repetitions of these operations were adjusted based on image distance. For example, at 1 m distance, dilation and closing were applied four times, while for 60 m and 100 m distances, one iteration was sufficient. A kernel size of 25 × 25 was used for both LDHF-DB and Tuft datasets.

An ablation study was conducted to evaluate the impact of different structuring element shapes (square, disk, and ellipse) and kernel sizes (15×15, 25×25, and 35×35). The results show that a 25×25 square element provides the best trade-off between noise removal and detail preservation, improving mean IoU by 6–8% compared to smaller kernels.

F. Masking

The refined binary mask obtained from morphological processing was combined with the ground truth facial image through a masking process, ensuring that only the relevant facial region was preserved for evaluation [22]. It is important to note that the ground-truth masks were used solely for evaluation purposes, not during detection or segmentation. The predicted mask obtained from morphology was compared against the ground-truth mask to compute performance metrics, ensuring that no ground-truth information was leaked into the detection process.

G. Performance Evaluation

The performance was quantitatively assessed using the Peak Signal-to-Noise Ratio (PSNR). Higher PSNR values indicate better similarity between the processed image and the ground truth, while values below 30 dB suggest poor image quality [23][24]. Comparisons were made before and after applying morphological operations to evaluate their effectiveness. The PSNR value can be expressed by the following equation [25]:

$$PSNR = 20\left(\frac{F_{max}}{\sqrt{MSE}}\right) \tag{1}$$

Where:

F_{max} = 255 for 8-bit image

All experiments were conducted using Python 3.10, OpenCV 4.9, and dlib 19.24 on a machine with an Intel Core i7-12700H CPU and 16 GB RAM. The LDHF-DB and Tufts datasets were split into 80% training and 20% testing sets. Random seeds were fixed at 42 for reproducibility. The implementation scripts and configuration files will be made publicly available upon publication.

III. RESULTS AND DISCUSSIONS

The experimental evaluation was conducted on NIR images from the LDHF-DB and Tuft datasets at varying distances of 1 m, 60 m, and 100 m. The results are presented in terms of the face detection output, thresholding, morphological operations, masking, and quantitative performance evaluation using PSNR.

A. Face Detection

The initial stage employed the HOG + SVM detector to identify facial landmarks and generate bounding boxes. Figure 4 illustrates the bounding box results of face detection on NIR images from the LDHF-DB dataset at distances of 1 m, 60 m, and 100 m. At 1 m, the bounding boxes clearly localize the face with high accuracy and visible facial details. At 60 m, the system still detects the face correctly, although the sharpness decreases compared to shorter distances. At 100 m, face detection remains possible but with lower image clarity and reduced facial detail, indicating that longer distances pose greater challenges for reliable detection.

Figure 5 presents the bounding box results of face detection on the Tuft dataset. Similar to the LDHF-DB results, the method successfully identifies and localizes the face region in NIR images. However, compared to LDHF-DB, the Tuft dataset shows more variation in facial poses and conditions, which makes detection more challenging. Despite these variations, the bounding boxes demonstrate that the proposed method is capable of consistently detecting faces across different datasets.

As illustrated in Figures 4 and 5, the bounding boxes successfully localized faces across all image distances in both datasets. However, challenges were observed at longer distances (100 m), where several faces were not detected due to reduced image clarity.
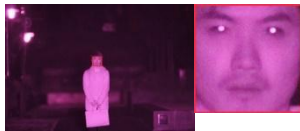
B. Thresholding

Subsequent processing using Otsu's thresholding produced binary images by separating the foreground (face) from the background. Figure 6 shows the Otsu thresholding results on NIR images from the LDHF-DB dataset at distances of 1 m, 60 m, and 100 m. The thresholding step successfully separates the facial region from the background, although some non-facial areas remain, particularly at longer distances. Figure 7 presents the Otsu thresholding results for the Tuft dataset. Similar to LDHF-DB, the method highlights the face region, but variations in facial appearance and background introduce more noise, indicating the need for further refinement.
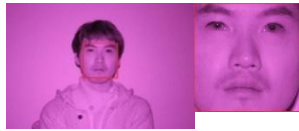
a. Image bounding box result NIR distance 1 meter

a. Image bounding box result NIR distance 60 meters

b. Image bounding box result NIR distance 100 meters

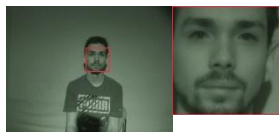Fig. 4. Bounding box result of the image NIR dataset LDHF-DB.

Fig. 5. Bounding box result of the image NIR dataset Tuft.

a. Image Otsu threshold result NIR distance 1 meter

b. Image Otsu threshold result NIR distance 60 meters

c. Image Otsu threshold result NIR distance 100 meters

Fig. 6 Otsu threshold result of the image NIR dataset LDHF-DB.

Fig. 7. Otsu threshold result of the image NIR dataset Tuft.

C. Morphological Operations

To refine the segmentation results, morphological operations (dilation and closing) were applied. As shown in Figures 8 and 9, these operations successfully enhanced the continuity of facial regions, removed small holes, and reduced background noise. The number of repetitions was adapted to the image distance, with closer images requiring more iterations than distant ones.
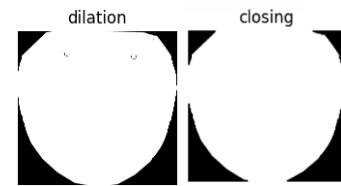
a. Image morphology result NIR 1 meter distance
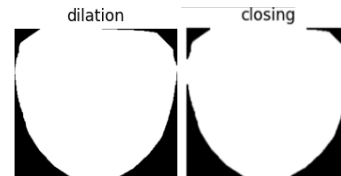
b. Image morphology result NIR 60-meter distance
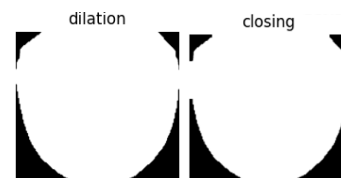
c. Image morphology result NIR 100-meter distance

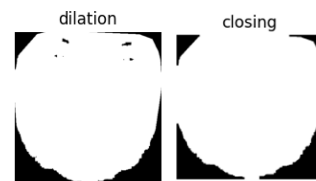Fig. 8. Image morphology result NIR dataset LDHF-DB.

Fig. 9. Image morphology result NIR dataset Tuft

D. Masking

The refined binary masks were then combined with the ground-truth images through masking. Figure 10 illustrates the masking results on NIR images from the LDHF-DB dataset at distances of 1 m, 60 m, and 100 m. The masking process combines the refined binary mask obtained from morphological operations with the ground-truth image, allowing only the facial region to be preserved. This step effectively eliminates residual background areas and improves the clarity of the segmented face, particularly at shorter distances where image quality is higher. Figure 12 presents the masking results on NIR images from the Tuft dataset. Despite greater variation in facial appearance and environmental conditions compared to LDHF-DB, the masking process successfully isolates the face region while removing non-facial areas. This demonstrates the robustness of the proposed approach in handling different datasets and improving the localization of facial regions for subsequent evaluation. It concludes that this process effectively preserved only the facial regions, improving segmentation quality compared to the initial thresholding results.

a. Image masking result NIR distance 1 meter

b. Image masking result NIR distance 60 meters

c. Image masking result NIR distance 100 meters

Fig. 10. Masking result of the image NIR dataset LDHF-DB.

Fig. 11. Masking result of the image NIR dataset Tuft.

Table 1 summarizes the results of face detection on NIR images from the LDHF-DB dataset at three different distances: 1 m, 60 m, and 100 m. At distances of 1 m and 60 m, all 100 images were successfully detected, yielding a 100% detection accuracy. However, at 100 m, only 84 out of 100 images were detected, resulting in an accuracy of 84%. This indicates that face detection performance is highly reliable at shorter distances but declines significantly when the capture distance increases due to reduced image clarity and noise interference. Table 2 presents the detection results on the Tuft dataset. From a total of 60 images, all faces were successfully detected, achieving a 100% detection accuracy. These results demonstrate the capability of the proposed method to consistently detect faces across different datasets. When compared with the LDHF-DB dataset, the Tuft results reinforce that distance plays a key role in detection reliability, with shorter ranges providing superior accuracy.

TABLE 1. FACE DETECTION RESULTS ON THE LDHF-DB DATASET AT DIFFERENT CAPTURE DISTANCES (1 M, 60 M, AND 100 M)

No	Image Distance	Number of Images	
		Detected	Not Detected
1	Image NIR at a distance of 1 meter	100	0
2	Image NIR at a distance of 60 meters	100	0
3	Image NIR at a distance of 100 meters	84	16

TABLE 2: FACE DETECTION RESULTS ON THE TUFT DATASET

No	Number of Images	
	Detected	Not Detected
1	60	0

E. Performance Evaluation using PSNR

The effectiveness of the proposed method was quantitatively assessed using the Peak Signal-to-Noise Ratio (PSNR), which measures the similarity between the processed image and the ground truth. A higher PSNR value indicates better image quality and more accurate segmentation, while values below 30 dB are generally considered to represent poor quality. Figures 12–15 show the histogram distribution of PSNR values for NIR images from the LDHF-DB and Tuft datasets at different distances. The results demonstrate that the proposed approach consistently achieves PSNR values above 30 dB after applying morphological operations, confirming the improvement in segmentation accuracy. For the LDHF-DB dataset, the 1 m images achieved the highest PSNR values, followed by 60 m and 100 m. This indicates that closer capture distances yield better face localization and higher image quality. The Tuft dataset also showed consistently high PSNR values, further validating the robustness of the method across different datasets.
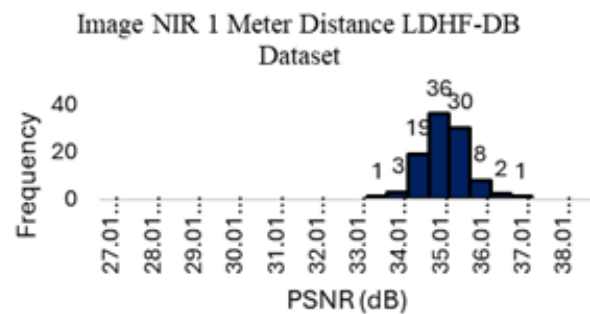

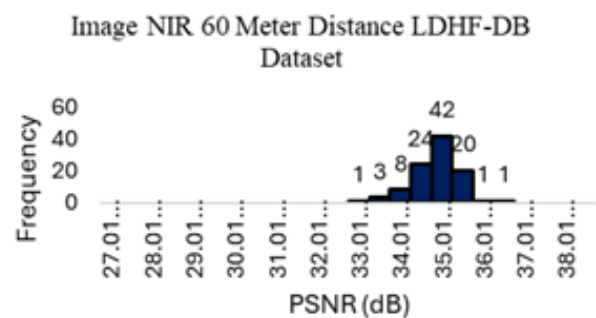Fig. 12. Histogram of PSNR image NIR distance 1-meter LDHF-DB dataset.

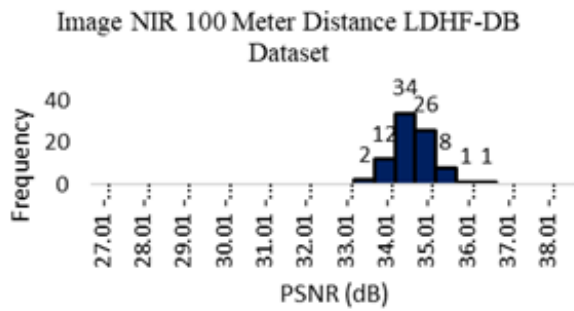Fig. 13. Histogram of PSNR image NIR distance 60-meter LDHF-DB dataset.

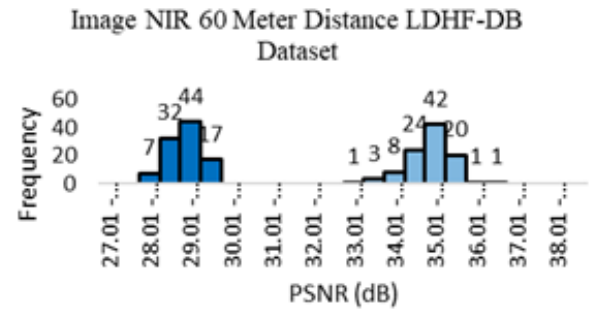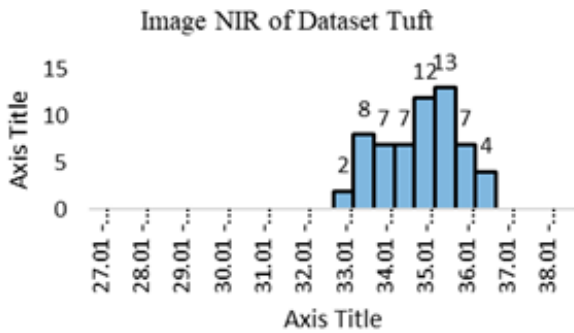Fig. 14. Histogram of PSNR image NIR distance 100-meter LDHF-DB dataset

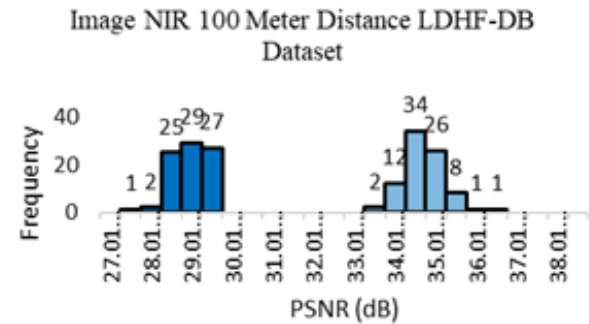Fig.15. Histogram of PSNR image NIR of the Tuft dataset

F. Comparison Before and After Morphology

A comparison of PSNR values before and after applying morphology is presented in Figures 16–19. Before morphology, most images recorded PSNR values below 30 dB, reflecting incomplete segmentation and the presence of noise or background artifacts. After morphology, PSNR values increased significantly, with an average improvement of more than 35%, demonstrating the effectiveness of dilation and closing in refining facial segmentation. Overall, the PSNR evaluation confirms that combining NIR imagery with morphological processing substantially enhances face detection performance, particularly in low-light conditions and at shorter capture distances. However, detection at longer distances (100 m) remains challenging, suggesting the need for further optimization to handle image degradation and noise.
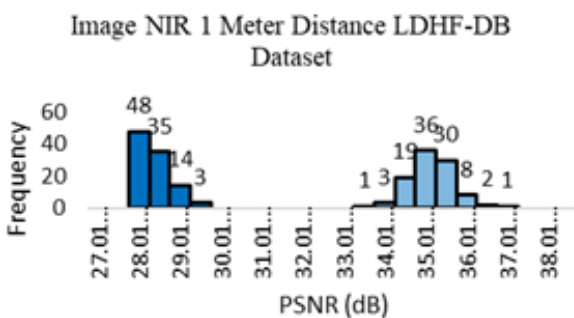

Fig. 16. Histogram of PSNR image NIR dataset LDHF-DB distance 1 meter.

Fig. 17. Histogram of PSNR image NIR dataset LDHF-DB distance 60 meters.

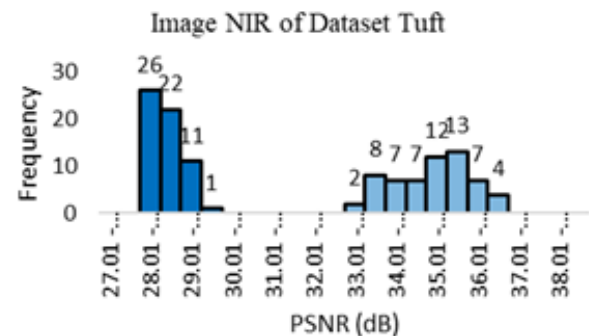Fig. 18. Histogram of PSNR image NIR dataset LDHF-DB distance 100 meters.

Fig. 19. Histogram of PSNR image NIR of the Tuft dataset.

IV. ETHICAL AND SOCIETAL CONSIDERATIONS

The deployment of NIR- or thermal-based face detection systems raises important ethical and societal issues. These include privacy, consent, and the potential misuse of surveillance data. The authors acknowledge these concerns and emphasize that the proposed system is intended for controlled environments and security applications where consent and data protection regulations are enforced. Future work will consider fairness across demographic groups and incorporate bias mitigation strategies to ensure ethical use.

V. CONCLUSION

This study demonstrated that integrating NIR thermal imaging with morphological operations significantly improves the accuracy and robustness of face detection under low-light conditions. Using the LDHF-DB and Tuft datasets at varying distances (1 m, 60 m, and 100 m), the results showed that morphological processing (dilation and closing)

effectively refined segmentation by removing non-facial regions and preserving essential facial structures. The performance evaluation using PSNR confirmed a substantial improvement, with values consistently exceeding 30 dB after morphology, compared to values below 30 dB before processing. The highest performance was observed at the 1 m distance, while accuracy decreased with longer capture distances. Overall, the proposed approach highlights the potential of NIR spectrum imagery as a reliable alternative to visible-light-based detection, particularly in dark or unconstrained environments. For future work, this study can be extended by integrating deep learning models to further enhance detection accuracy, combining NIR with other spectral modalities for greater robustness, and optimizing the method for real-time applications in security and surveillance systems. Additional experiments will be conducted on NIR images containing occlusions such as eyeglasses and face masks to further evaluate the model's robustness under real-world conditions. Moreover, cross-dataset evaluation (e.g., training on LDHF-DB and testing on Tufts) will be extended to investigate domain generalization capabilities. These efforts aim to develop more adaptive and resilient models through cross-domain learning and improved feature normalization techniques.

DECLARATION OF GENERATIVE AI AND AI-ASSISTED TECHNOLOGIES IN THE WRITING PROCESS

During the preparation of this work, the author used *ChatGPT (OpenAI)* and *Grammarly* to assist with language refinement, grammar correction, and clarity of academic writing. After using these tools, the author thoroughly reviewed, verified, and edited the content as needed and takes responsibility for the integrity and accuracy of the published article.

REFERENCES

[1] P. Sonawane, H. Sirsath, P. Gadhakar, S. Khedkar, and S.A.Chiwhane, "Drunk Person Identification Using Thermal Infrared Images," International Journal of Advanced Research in Computer Communication Engineering, vol. 7, no. 5, pp. 181–184, 2018, doi: 10.1504/IJESDF.2012.049747.

[2] D. N. Parmar and B. B. Mehta, "Face Recognition Methods & Applications," International Journal of Computer Technology & Applications, vol. 4, no. 1, p. 1, 2013.

[3] J. B. Dowdall, I. Pavlidis, and G. Bebis, "Face Detection in the Near-IR Spectrum," Journal of Image and Vision Computing, vol. 21, no. 7, p. 565, 2003, doi: 10.1016/S0262-8856(03)00055-6.

[4] Julham, S. S. T. Hutagalung, K. C. Simalango, and S. Lumbantobing, "The Effectiveness of OpenCV-Based Face Detection In Low-Light Environments," Journal of Informatics and Telecommunication Engineering, vol. 7, no. 1, p. 209, 2023, doi: 10.31289/jite.v7i1.9851

[5] H. Mohsin and S. H. Abdullah, "Human Face Detection using Skin Color Segmentation and Morphological Operations," Journal of Al-Nisour University College, vol. 7, p. 63, 2018.

[6] Y. Kang and W. Pan, "A Novel Approach of Low-Light Image Denoising for Face Recognition," Advances in Mechanical Engineering, vol. 6, 2014, doi: 10.1155/2014/256790.

[7] A. Gyaourova, G. Bebis, and I. Pavlidis, "Fusion of Infrared and Visible Image for Face Recognition," European Conference on Computer Vision, pp. 456–468, 2004, doi: 10.1007/978-3-540-24673-2_37.

[8] B. Martinez, X. Binefa, and M. Pantic, "Facial Component Detection in Thermal Imagery," in IEEE Conference Computer Society Conference, European, 2010, pp. 48–54, doi: 10.1109/CVPRW.2010.5543605.

[9] L. L. Chambino, J. S. Silva, and A. Bernardino, "Multispectral Facial Recognition : A review," in IEEE Access, vol. 8, 2020, doi: 10.1109/ACCESS.2020.3037451.

[10] E. Bishoff, C. Godfrey, M. McKay, and E. Byler, "Quantifying the Robustness of Deep Multispectral Segmentation Models Against Natural Perturbations and Data Poisoning," 2023, doi: 10.1117/12.2663498.

[11] T. Bourlai and B. Cukic, "Multi-Spectral Face Recognition: Identification of People in Difficult Environments," Algorithms, Technologies, and Applications for Multispectral and Hyperspectral Imaging XXIX Conference, 2012.doi: 10.1109/ISI.2012.6284307.

[12] H. Fitriyah and E. R. Widasari, "Face Detection of Thermal Imaging in Various Standing Body-Pose using Facial Geometry," Indonesian Journal of Computing and Cybernetics Systems, vol. 14, no. 4, pp. 407–416, 2020.doi: 10.22146/ijccs.59672.

[13] M. Kristo and M. Ivasic-Kos, "An Overview of Thermal Face Recognition Methods," in 41st International Convention on Information and Communication Technology, Electronics and Microelectronics, 2018, p. 5, doi: 10.23919/MIPRO.2018.8400200

[14] E.Stach, "Structural Morphology and Self-Organization," in Conference: Design and Nature, 2010, vol. 138, p. 30, doi : 10.2495/DN100041

[15] D. Kang, H. Han, A. K. Jain, S.W. Lee, "Nighttime face recognition at large standoff: Cross-distance and cross-spectral matching." Pattern Recognition, vol. 47, pp. 3750–3766, 2014, doi: 10.1016/j.patcog.2014.06.004

[16] K. Panetta, G. Chen, S. Rajeev, S. Agaian, Y. Zhou, and S. Wei, "A Comprehensive Database for Benchmarking Imaging Systems," IEEE Transactions on Pattern Analysis and Machine Intelligence, vol. 40, no. 5, pp. 1051–1065, 2018, doi: 10.1109/TPAMI.2018.2884458.

[17] J. M. S. Waworundeng and R. R. I. Suwu, "Implementation of Face Recognition in People Monitoring Access In-and-Out of Crystal Dormitory Universitas Klabat," Cogito Smart Journal, vol. 9, no. 1, p. 159, 2023, doi: 10.31154/cogito.v9i1.500.156-170

[18] S. Sunardi, A. Fadlil, and D. Prayogi, "Face Recognition Using Machine Learning Algorithm Based on Raspberry Pi 4b," International Journal of Artificial Intelligence Research, vol. 6, no. 1, 2022, doi: 10.29099/ijair.v7i1.321

[19] M. P. Damayanti and H. Sumarti, "Analysis of Axial CT-Scan Image of COVID-19 Patients Based in Gender using the Otsu Thresholding Method," Journal of Natural Sciences and Mathematics Research, vol. 6, no. 1, p. 7, 2020.

[20] A. M. Raid, W. M. Khedr, M. A. El-dosuky, and M. Aoud, "Image Restoration Based on Morphological Operations," International Journal of Computer Science, Engineering and Information Technology, vol. 4, no. 3, pp. 10–11, 2014, doi: 10.5121/ijcseit 2014.4302

[21] K. Sreedhar and B. Panlal, "Enhancement of Images Using Morphological Transformations," International Journal of Computer Science & Information Technology, vol. 4, no. 1, p. 38, 2012, doi: 10.5121/ijcsit.2012.4103

[22] D. Dussol, P. Druault, B. Mallat, and S. Delacroix, "Automatic Dynamic Mask Extraction for PIV Images Containing an Unsteady Interface, Bubbles, and a Moving Structure," Comptes Rendus Mécanique, vol. 344, no. 7, p. 470, 2016, doi: 10.1016/j.crme.2016.03.005

[23] A. B. Prasetyo et al., "Comparative Analysis of Image on Several Edge Detection Techniques," Journal of Technology Education Management Informatics, vol. 12, no. 1, p. 111, 2023, doi: 10.18421/TEM121-15

[24] E. J. Leavline and D. A. A. G. Singh, "Salt and Pepper Noise Detection and Removal in Gray Scale Images : An Experimental Analysis," International Journal of Signal Processing, Image Processing and Pattern Recognition, vol. 6, no. 5, p. 347, 2013, doi: 10.14257/ijsip.2013.6.5.30

[25] B. U. Fahnun, A. B. Mutiara, J. Harlan, and E. P. Wibowo, "Feature Identification of Hepatic Cancer Ultrasound Image using Gaussian Filtering Combined with Intensity Adjustment," International Journal of Engineering Research & Technology, vol. 8, no. 9, p. 517, 2019, doi:10.17577/IJERTV8IS090137.